The Active Encounter Complex in Frustrated Lewis Pair Chemistry

Alastair T. Littlewood[1], Tao Liu[2], Linjiang Chen[1], Timothy A. Barendt*[1], Andrew R. Jupp*[1]

[1]: School of Chemistry, University of Birmingham, Edgbaston, Birmingham, B15 2TT, UK

[2]: Department of Chemistry, University of Liverpool, Liverpool, L69 7ZD, UK.

*: Corresponding authors: t.a.barendt@bham.ac.uk, a.jupp@bham.ac.uk

---

Abstract: Sustainable catalysts based on main-group elements have emerged as alternatives to expensive and environmentally unfriendly precious metal systems. Frustrated Lewis pairs (FLPs) are precluded from forming a classical Lewis adduct, and have displayed remarkably versatile reactivity in the fields of small-molecule activation and catalysis. The initial reaction of the acid, base and small molecule (*e.g.* H_2) is formally termolecular, but the viability of this reaction is rationalised by the pre-association of the acid and base in an encounter complex. However, there is no experimental methodology to study the active encounter complex, *i.e.* the pre-associated complex that is in the correct orientation for small-molecule activation. Here we show that the charge-transfer band between $PMes_3$ and $B(C_6F_5)_3$ can be analysed by supramolecular techniques to provide the key thermodynamic parameter, K_a, for the active encounter complex. We also demonstrate that a higher concentration of active encounter complex in solution leads to a faster activation of hydrogen. This method enables researchers to directly probe the complex that underpins FLP small-molecule activation and subsequent catalysis, and will aid the design of more active sustainable catalysts.

There is a huge drive to develop new sustainable chemical reactions fit for the 21st century. Frustrated Lewis pairs (FLPs) have emerged as a versatile class of main-group catalysts for a wide range of reactions and applications.[1, 2, 3, 4, 5, 6] FLPs are systems that comprise Lewis acids and bases that, due to bulky substituents, are precluded from forming a Lewis adduct; the latent reactivity of these unquenched acidic and basic sites can be exploited for the cooperative activation of small molecules, including the heterolytic cleavage of dihydrogen, H_2. The resulting proton and hydride can subsequently be delivered to a wide range of unsaturated organic substrates, such as alkenes, imines, and ketones, to promote the catalytic reduction of these functional groups without the need for precious metals (Fig. 1).[7, 8, 9] The scope of FLP chemistry continues to grow, with applications in C–H activation,[10] asymmetric catalysis,[11, 12] heterogeneous catalysis,[13, 14, 15] and polymer synthesis.[16, 17]

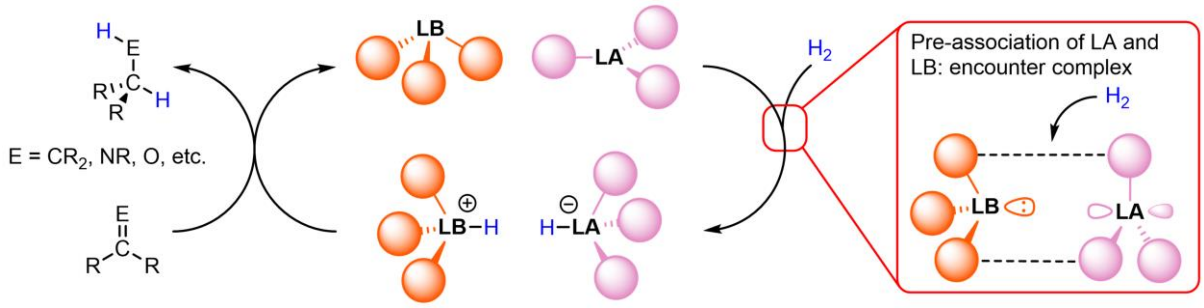

Fig. 1: General catalytic cycle for FLP hydrogenation catalysis with generic three-coordinate Lewis base (LB) and Lewis acid (LA), highlighting the crucial role of the encounter complex stabilised by dispersion interactions.

The first step in the catalytic cycle of FLP hydrogenation is the splitting of H_2 by the FLP (Fig. 1). For archetypal intermolecular FLPs, this step involves the apparent simultaneous collision of three distinct molecules: the Lewis acid, the Lewis base, and H_2. The rationale to explain this termolecular reactivity is the pre-association of two of the components. For H_2 activation by a phosphine and a borane, it has been shown that the Lewis acid and base form a weakly-bound species called the "encounter complex", which features a reactive pocket into which a molecule of H_2 can diffuse.[18] The encounter complex was first proposed by Pápai and co-workers in a computational study, where they identified a weakly associated $[P(^tBu)_3]\cdots[B(C_6F_5)_3]$ adduct as a minimum on the potential energy surface.[19] They showed that the encounter complex is not held together by a classical P→B dative bond, but instead by a large number of individually weak C–H···F non-covalent interactions. These C–H···F interactions for a range of FLP systems were corroborated by non-covalent interaction (NCI) analysis.[20, 21] The favourable stabilisation energy in FLP systems is significant (approximately 10-15 kcal mol^{-1}), and the inclusion of implicit solvent corrections only slightly reduces this stabilisation.[22] However, the enthalpic stabilisation is opposed by the entropic cost of adduct formation, and this is consistent with difficulties in observing the encounter complex experimentally.[18, 23]

Compelling evidence for its formation in solution was provided by $^{19}F,^{1}H$ HOESY (Heteronuclear Overhauser Enhancement Spectroscopy) experiments performed on concentrated (220-230 mM) samples of $P(^tBu)_3/B(C_6F_5)_3$ or $PMes_3/B(C_6F_5)_3$ in toluene or benzene, where cross-peaks corresponding to H···F interactions could be observed.[24] Interestingly, the data showed that there are interactions between all fluorine environments on the borane and all proton environments on the phosphine, indicating that the two components are randomly oriented within the encounter complex in solution. The lack of preference for a particular configuration was supported by further high-level computations, which showed that the two "extreme" configurations shown in Fig. 2 are very similar in energy (< 1 kcal mol^{-1} difference for $PMes_3/B(C_6F_5)_3$).[25] There is currently no method that can probe the "active encounter complex" (see Fig. 2a) in solution, *i.e.* where the Lewis acid and base components are oriented in the correct manner for small-molecule activation and subsequent catalysis.

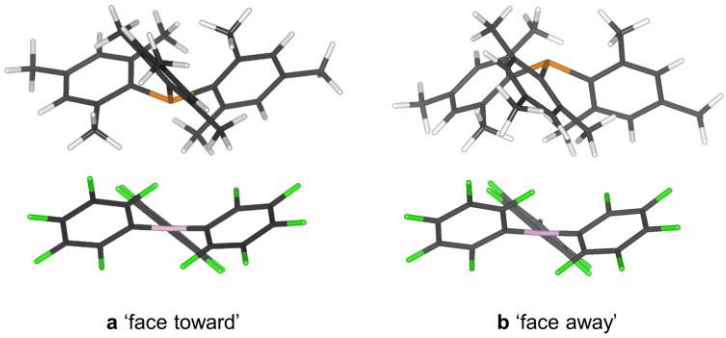

Fig. 2: Optimised structures of the two extreme forms of the encounter complex comprising $PMes_3$ and $B(C_6F_5)_3$. Calculations carried out at the B97D3(BJ)/Def2SVP level of theory.

Supramolecular chemistry has developed the tools with which to study interacting molecules, an important aspect being to quantify the binding strength of a non-covalent complex by measuring the association constant, K_a. Knowledge of K_a enables the design of supramolecular complexes with tuneable affinities, which has proven critical for applications across chemical sensing,[26] sequestration,[27] and catalysis.[28] The only previous attempt to quantify the K_a of an FLP encounter complex experimentally was that of $PMes_3/B(C_6F_5)_3$ in deuterated benzene; the method consisted of using diffusion ordered ^1H and ^{19}F NMR spectroscopy (DOSY) to determine the hydrodynamic radii for a small series of $PMes_3$:$B(C_6F_5)_3$ ratios.[24] These hydrodynamic radii were compared to the free species ($PMes_3$ and $B(C_6F_5)_3$) to predict a mole fraction of the encounter complex and ultimately an estimation of $K_a = 0.5 \pm 0.2\ M^{-1}$. Alongside a number of assumptions to approximate the hydrodynamic radii, this approach required an adapted NMR single-point method to estimate K_a, which is considered to be less accurate than fitting a supramolecular titration curve through non-linear regression.[29] A very recent article determined the association constants of dispersion-stabilised Lewis pairs comprising phosphines and boranes, but these adducts featured P–B dative bonds and are thus fundamentally different to the "frustrated" system described here.[30]

For the first time, we quantify FLP association using a UV-vis spectroscopic titration, a methodology that enables us to determine K_a by accurate non-linear curve fitting,[31] the gold standard in supramolecular chemistry.[29] This strategy provides the first experimental probe for the "active encounter complex" of an FLP in solution, an outcome that is supported by an extensive computational study into the relative orientations of $PMes_3$ and $B(C_6F_5)_3$ in the encounter complex. We have used these results to show for the first time that a higher concentration of active encounter complex in solution leads to faster small-molecule activation. The fundamental understanding of the encounter complex we uncover here will facilitate the design of more active FLPs.

Results

$PMes_3$ and $B(C_6F_5)_3$ are both colourless when independently dissolved in toluene, but the combination of the two gives rise to a magenta colour (see Fig. 3, S1 and S2). This fact has been documented since the earliest report of this system being used as an FLP,[32] but it was only recently determined that this colour arises from the formation of a charge-transfer complex

between the Lewis acid and base.[33, 34] The charge-transfer band with λ_{max} = 534 nm enabled us to directly measure the association constant (K_a) of the Lewis acid and base of an FLP in toluene solution (Fig. 3a). The $PMes_3/B(C_6F_5)_3$ complex is air- and moisture-sensitive; the pale magenta colour in solution begins disappearing immediately upon exposure to standard atmospheric conditions (Fig. S23). This necessitated that all samples were prepared and analysed after equilibration in an N_2-filled glovebox. To determine K_a,[31] 13 discrete solutions of $PMes_3/B(C_6F_5)_3$ were prepared under inert conditions with a constant concentration of the Lewis acid (5 mM), and increasing concentrations of Lewis base (up to 300 mM, *i.e.* 60 equivalents). As expected, increasing the Lewis base:acid ratio led to an increase in intensity of the magenta colour, which is clearly visible to the naked eye (Fig. 3b). The intensity of the charge-transfer absorption band at λ_{max} = 534 nm was measured by UV-vis spectroscopy (Fig. 3c), and showed the characteristic increase before levelling off at higher concentrations of phosphine (Fig. 3d). The K_a value was calculated by non-linear fitting of the resulting titration curve to a 1:1 stoichiometric binding model.[29, 35] Titrations were carried out in triplicate (with separate samples prepared each time), to give an average K_a of 2.52 M^{-1} with a relative standard deviation of 0.43 M^{-1} for the FLP $PMes_3/B(C_6F_5)_3$. This average value corresponds to ΔG = –0.55 kcal mol^{-1} for the association of the acid and base in toluene at 298 K; this very low value is consistent with previous computational reports that the encounter complex will only be present in low concentration in solution,[20, 22, 25] although it does highlight that association is a very slightly exothermic process.

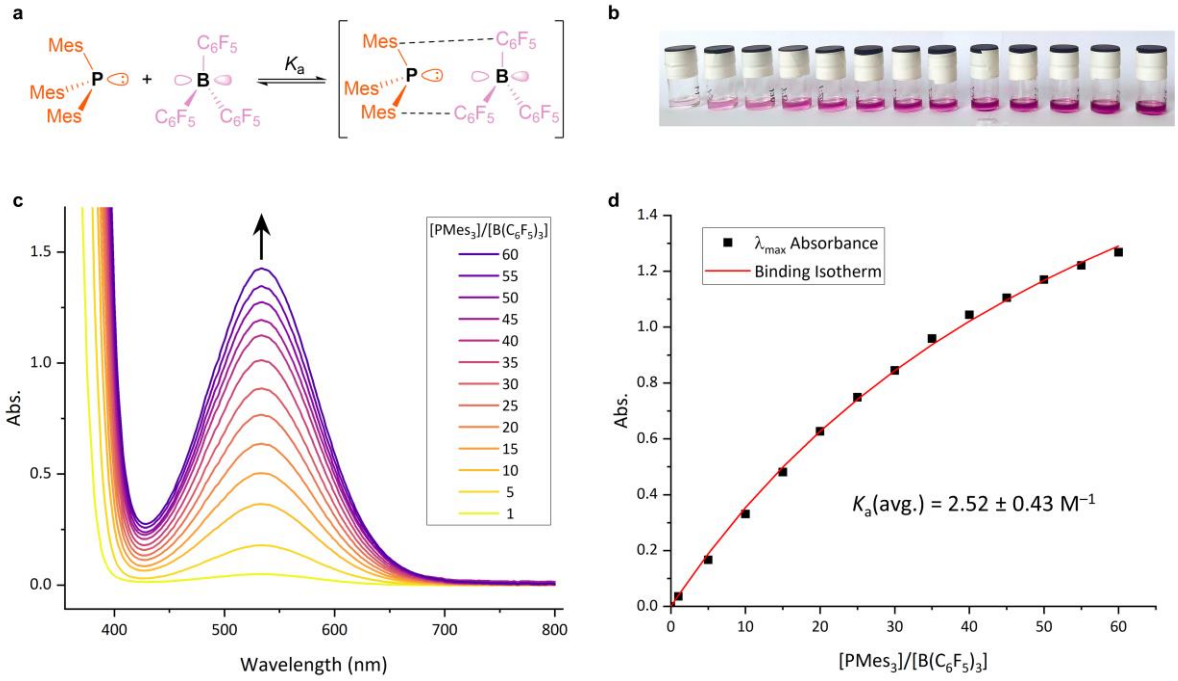

Fig. 3: **a**: Complexation for which K_a is being determined. **b**: Solutions used in titration experiments; increasing magenta colour with increasing ratios of phosphine:borane. **c**: Increasing λ_{max} of charge-transfer band with increasing Lewis base concentration. **d**: plot of λ_{max} absorbance as a function of phosphine:borane ratio, and the binding isotherm that has been modelled to fit these data.

Computational Analysis

There are many possible orientations of the associated acid and base within the encounter complex, and previous experimental efforts to characterise the encounter complex have only been able to show that the two components are associated, but without any differentiation between the relative orientations.[18] Many of these orientations could generate a charge-transfer band and thus enable SET due to the overlap of various donor and acceptor orbitals on the phosphine and borane, respectively, such as π–π* transitions due to π-stacking interactions of the aryl rings on the phosphine and borane.

We hypothesised that our UV-vis spectroscopic probe is sensitive only to the active encounter complex, *i.e.* the orientation that is correctly set up for small-molecule activation. Our hypothesis was based on the fact that the HOMO of the $PMes_3/B(C_6F_5)_3$ combination is predominantly the lone pair on P and the LUMO is the formally vacant p orbital on B.[34] Therefore, alignment of these frontier orbitals would presumably permit the lowest energy SET process, which would correlate to the charge-transfer absorption band monitored in the supramolecular titration (Fig. 3c). We therefore sought to probe this chemical space in a systematic and rigorous manner to determine the source of our diagnostic charge-transfer band.

We explored a wide range of possible orientations for the acid and base within the encounter complex, beyond the two extremes in Fig. 2. The input coordinates for the $PMes_3/B(C_6F_5)_3$ encounter complexes were generated in two ways (grid search and scanning method), and 1644 different permutations were used to explore the chemical space as comprehensively as possible (Fig. 4a); full details can be found in the SI. All 1644 input orientations were fully geometry-optimised and their energies calculated using the semi-empirical GFN2-xTB method (Fig. 4b).[36] By applying a cut-off of 5 kcal mol^{-1} above the global energy minimum on the xTB binding energy landscape (Fig. 4b), 810 $PMes_3/B(C_6F_5)_3$ binding configurations were selected and further geometry-optimised using density functional theory (DFT: B97D3(BJ)/Def2-SVP),[37, 38, 39] of which 774 converged successfully. The binding energies of the optimised 774 configurations were determined by single-point energy calculations at the ωB97XD/Def2-TZVP level of theory,[39, 40] and this binding energy landscape is shown in Fig. 4c. These data show that there are many energetically accessible orientations, consistent with the aforementioned NMR spectroscopy experiments by Rocchigiani and co-workers.[24] Reassuringly, the binding energies of the two extreme orientations (Fig. 2) are very similar (–10.285 and –10.287 kcal mol^{-1}), in good agreement with the previous calculations performed by Grimme and co-workers.[25]

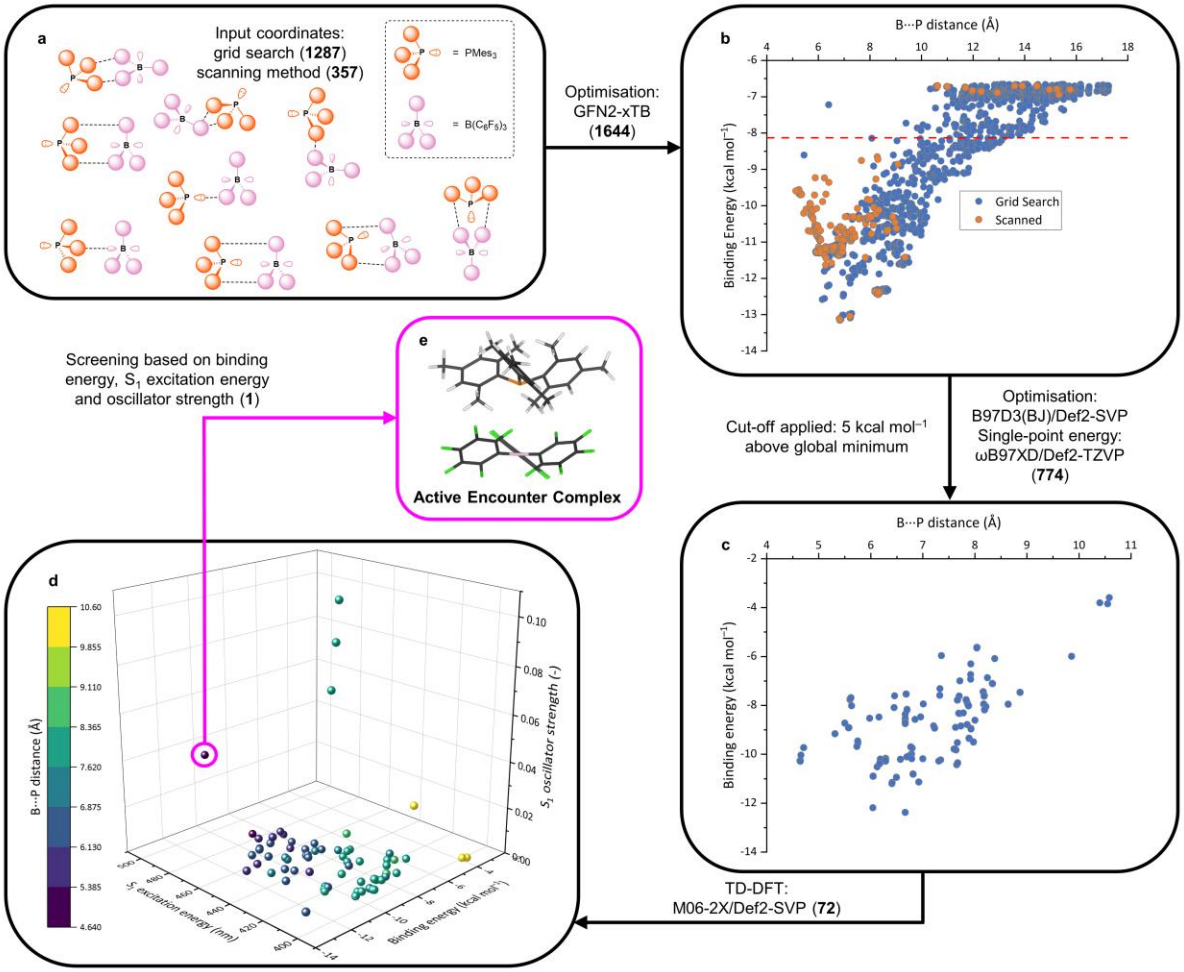

Fig. 4: Flowchart of computational study on the active encounter complex. The numbers in bold show how many configurations are being carried through the workflow at each stage. **a**: Schematic representations of some of the 1644 input coordinates of the encounter complexes. **b**: Graph showing binding energy as a function of P···B distance calculated using a semi-empirical method. The cut-off of 5 kcal mol^{-1} above the global energy minimum is shown by a red dashed line, and all points above this line were discarded. **c**: Graph showing binding energy as a function of P···B distance, calculated using DFT; the 774 data points have converged to 72 distinct clusters. **d**: Three-dimensional plot comparing the binding energy with the S_1 excitation energies and oscillator strengths from TD-DFT. The range of P···B distances for each point is also indicated by the colour chart. **e**: The structure of the only data point that has values from the plot in **d** that is consistent with the experimentally observed absorbance band; the active encounter complex.

The lowest energy transitions within these different optimised orientations were calculated using time-dependent DFT (TD-DFT). The lowest energy orientation from each cluster was used to create a set of 72 representative configurations, and the vertical excitation for each configuration was simulated at the TD-M062X/Def2-SVP level of theory.[39, 41] These data allowed us to compare the three separate criteria: binding energies, S_1 transition energies, and respective oscillator strengths (Fig. 4d).

The only combination of the three parameters that is consistent with the experimentally observed transition is the point depicted in Fig. 4e, which features the transition with the lowest S_1 transition energy (499 nm, in reasonable agreement with the experimental value of 534 nm), a relatively significant oscillator strength, and a binding energy close to the global minimum. This data point corresponds to the orientation where the phosphine lone pair is pointing directly at the formally vacant p orbital on the borane, *i.e.* the orientation depicted in Fig. 2a. The majority of the calculated transitions (57 of the 72) have negligible oscillator strengths (<0.005) and thus these orientations are highly unlikely to contribute to the experimental absorbance band. The three transitions with the highest oscillator strengths (labelled α, β, and γ in Fig. S35 and S36) all arise from similar orientations that feature π-stacking interactions between one mesityl ring on the phosphine and one C_6F_5 ring on the borane, but these three orientations are relatively higher in energy than the other orientations and are thus also unlikely to have any appreciable contribution to the absorbance band.

This result reveals that our UV-vis spectroscopic titration method enables us to quantify the active encounter complex in solution, experimentally providing the key thermodynamic parameter for the first time on the weakly associated species in solution that underpins FLP small-molecule activation and subsequent catalysis.

Hydrogen Activation Studies

Knowledge of the K_a of the active encounter complex enables accurate mole-fractions to be determined; for example, using the average K_a of 2.52 M^{-1}, a 1:1 mixture of $PMes_3/B(C_6F_5)_3$ at 5 mM concentration in toluene (which matches the concentration of our UV-vis titrations) would result in 1.2% of the components being in the active encounter complex at any moment. This low percentage could partially explain why FLP catalysts have relatively low activity compared to transition metal systems, as in this case 98.8% of the catalyst is not in its active form at any one time. But by increasing the relative ratio of $PMes_3$ to $B(C_6F_5)_3$ to 10:1, 11.1% of the limiting borane would be in the active encounter complex in solution. It is therefore possible to significantly increase the amount of active catalyst by simply increasing the amount of only one component (the Lewis base in this case), which also has economic advantages as the Lewis acid $B(C_6F_5)_3$ is typically the more expensive component within the FLP.

We sought to experimentally verify this prediction by studying the rate of hydrogen activation by the FLP as a function of encounter complex concentration (Fig. 5a). Two reactions were set up with $PMes_3/B(C_6F_5)_3$ ratios of 1:1 (**A**) and 10:1 (**B**), respectively, in toluene with the $B(C_6F_5)_3$ at 5 mM concentration, and a constant flow of H_2 was passed over the stirring reactions. As the FLP reacted with hydrogen to form the colourless salt $[HPMes_3]^+[HB(C_6F_5)_3]^-$, the magenta colour from the $PMes_3/B(C_6F_5)_3$ encounter complex became less intense. To make the kinetics of the reactions easier to follow, 5% H_2 in 95% N_2 carrier gas was used to slow down the rate of hydrogen activation. The intensity of the absorption band at 534 nm was monitored over time for the two reactions. The results in Fig. 5b clearly show that the loss of intensity is much faster for **B** than **A,** i.e., when there is a higher initial concentration of active encounter complex. In **A**, the reaction takes 88 minutes for the

absorption band to be at half its starting intensity, whereas this only takes 35 minutes for **B;** note this includes an induction period for the hydrogen to diffuse into solution. Subsequent ^{31}P, ^{19}F, and ^{11}B NMR analysis on samples from **A** and **B** was undertaken to corroborate the expected hydrogen activated products.

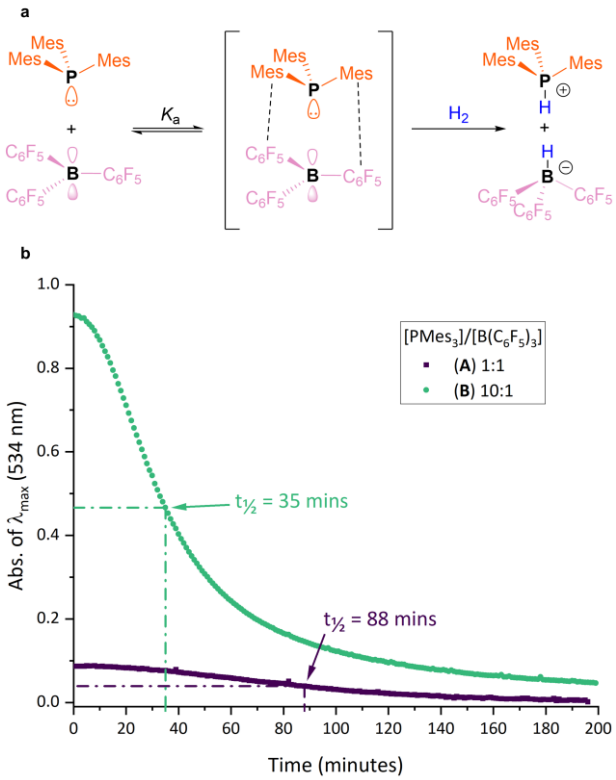

Fig. 5: **a**: H_2 activation by FLP being studied. **b**: Change in λ_{max} (534 nm) absorbance of 1:1 (black squares – reaction **A**) and 10:1 (blue circles – reaction **B**) ratios of $PMes_3/B(C_6F_5)_3$ under a flow of 5% H_2 & 95% N_2 as a function of time.

To quantify the extent of hydrogen activation by the FLP, reactions **A** and **B** were repeated and then stopped after 60 minutes by evacuating the reaction flask to prevent further reactivity. After removal of the toluene, the reaction samples were dissolved in $CDCl_3$ and analysed by quantitative ^{31}P NMR spectroscopic experiments (see SI for details), which revealed that 23% of the $PMes_3/B(C_6F_5)_3$ had been converted to $[HPMes_3][HB(C_6F_5)_3]$ in **A** after an hour, whereas the value was 41% for **B** (relative to the limiting reagent $B(C_6F_5)_3$). These experiments clearly show that a significant enhancement in reaction rates can be obtained by increasing the concentration of active encounter complex in solution.

Conclusions

We have developed a new methodology based on UV-vis spectroscopy to directly probe the encounter complex in frustrated Lewis pair chemistry, using the prototypical $PMes_3/B(C_6F_5)_3$ combination as an exemplar. We have employed best-practice techniques from supramolecular

chemistry to determine an average K_a of $PMes_3/B(C_6F_5)_3$ in toluene of 2.52 M^{-1}, which shows that the association of the Lewis acid and base is slightly favourable under these conditions. The in-depth computational study has thoroughly explored the chemical space of this encounter complex; starting with 1644 different input orientations, and using increasingly high-level computational methods we were able to show that the only configuration that is consistent with the charge-transfer absorbance band used in our spectroscopic titration is the orientation where the phosphorus lone pair is pointing at the formally vacant p orbital on boron. As this orientation is the same as that required for small-molecule activation, our methodology enables the first assessment of the key thermodynamic parameter of the active encounter complex that underpins FLP small-molecule activation and ensuing catalysis. We used the knowledge of the association constant and therefore mole-fraction of active encounter complex in solution to show that a higher concentration of active encounter complex leads to faster rate of hydrogen activation. This method unlocks the ability to assess the effects of experimental conditions on formation of the active encounter complex, for example the effects of different solvents, temperatures, and different FLP combinations and ratios, and enable the community to design more active main-group catalysts.

Author contributions

A.R.J. and T.A.B. designed the experiments. A.T.L conducted the experiments. A.T.L., T.A.B. and A.R.J. analysed experimental data. T.L. and L.C. conducted the computations. T.L., L.C. and A.R.J analysed the computational data. A.T.L. and A.R.J. wrote the manuscript with input from all authors.

Acknowledgements

A.T.L., L.C., T.A.B. and A.R.J. acknowledge the University of Birmingham for funding. A.R.J. would also like to thank the Royal Society (URF\R1\201636) for funding, and T.A.B. acknowledges the EPSRC (EP/W037661/1) for funding. Dr Cécile Le Duff is gratefully acknowledged for NMR spectroscopy discussions.

References

1. Welch GC, San Juan RR, Masuda JD, Stephan DW. Reversible, metal-free hydrogen activation. *Science* 2006, **314**(5802)**:** 1124-1126.

2. Stephan DW, Erker G. Frustrated Lewis pair chemistry: development and perspectives. *Angew Chem Int Ed* 2015, **54**(22)**:** 6400-6441.

3. Jupp AR, Stephan DW. New Directions for Frustrated Lewis Pair Chemistry. *Trends Chem* 2019, **1**(1)**:** 35-48.

4. Erker G, Stephan DW. *Frustrated Lewis Pairs I: Uncovering and Understanding*, vol. 332. Springer, Berlin, Heidelberg, 2013.

5. Erker G, Stephan DW. *Frustrated Lewis Pairs II: Expanding the Scope*, vol. 334. Springer, Berlin, Heidelberg, 2013.

6. Slootweg JC, Jupp AR. *Frustrated Lewis Pairs*, vol. 2. Springer: Switzerland, 2021.

7. Chase PA, Welch GC, Jurca T, Stephan DW. Metal-Free Catalytic Hydrogenation. *Angew Chem Int Ed* 2007, **46**(42)**:** 8050-8053.

8. Lam J, Szkop KM, Mosaferi E, Stephan DW. FLP catalysis: main group hydrogenations of organic unsaturated substrates. *Chem Soc Rev* 2019, **48**(13)**:** 3592-3612.

9. Stephan DW. Diverse Uses of the Reaction of Frustrated Lewis Pair (FLP) with Hydrogen. *J Am Chem Soc* 2021, **143**(48)**:** 20002-20014.

10. Légaré MA, Courtemanche MA, Rochette E, Fontaine FG. Metal-free catalytic C-H bond activation and borylation of heteroarenes. *Science* 2015, **349**(6247)**:** 513-516.

11. Meng W, Feng X, Du H. Frustrated Lewis Pairs Catalyzed Asymmetric Metal-Free Hydrogenations and Hydrosilylations. *Acc Chem Res* 2018, **51**(1)**:** 191-201.

12. Chen D, Klankermayer J. Metal-free catalytic hydrogenation of imines with tris(perfluorophenyl)borane. *Chem Commun* 2008(18)**:** 2130-2131.

13. Niu Z, Zhang W, Lan PC, Aguila B, Ma S. Promoting Frustrated Lewis Pairs for Heterogeneous Chemoselective Hydrogenation via the Tailored Pore Environment within Metal–Organic Frameworks. *Angew Chem Int Ed* 2019, **58**(22)**:** 7420-7424.

14. Ma Y, Zhang S, Chang CR, Huang ZQ, Ho JC, Qu Y. Semi-solid and solid frustrated Lewis pair catalysts. *Chem Soc Rev* 2018, **47**(15)**:** 5541-5553.

15. Jupp AR. Heterogeneous Catalysis by Frustrated Lewis Pairs. In: Slootweg JC, Jupp AR (eds). *Frustrated Lewis Pairs*. Springer, Cham, 2021, p 237−281.

16. Zhang Y, Miyake GM, Chen EY. Alane-Based Classical and Frustrated Lewis Pairs in Polymer Synthesis: Rapid Polymerization of MMA and Naturally Renewable Methylene Butyrolactones into High-Molecular-Weight Polymers. *Angew Chem Int Ed* 2010, **49**(52)**:** 10158-10162.

17. Hong M, Chen J, Chen EY. Polymerization of Polar Monomers Mediated by Main-Group Lewis Acid–Base Pairs. *Chem Rev* 2018, **118**(20)**:** 10551-10616.

18. Jupp AR. Evidence for the encounter complex in frustrated Lewis pair chemistry. *Dalton Trans* 2022, **51**(28)**:** 10681-10689.

19. Rokob TA, Hamza A, Stirling A, Soós T, Pápai I. Turning Frustration into Bond Activation: A Theoretical Mechanistic Study on Heterolytic Hydrogen Splitting by Frustrated Lewis Pairs. *Angew Chem Int Ed* 2008, **47**(13)**:** 2435-2438.

20. Skara G, Pinter B, Top J, Geerlings P, De Proft F, De Vleeschouwer F. Conceptual quantum chemical analysis of bonding and noncovalent interactions in the formation of frustrated Lewis pairs. *Chem Eur J* 2015, **21**(14)**:** 5510-5519.

21. Marques LR, Ando RA. Infrared Spectroscopy Evidence of Weak Interactions in Frustrated Lewis Pairs Formed by Tris(pentafluorophenyl)borane. *Chemphyschem* 2023, **24**(6)**:** e202200715.

22. Zeonjuk LL, Vankova N, Mavrandonakis A, Heine T, Röschenthaler GV, Eicher J. On the mechanism of hydrogen activation by frustrated Lewis pairs. *Chem Eur J* 2013, **19**(51)**:** 17413-17424.

23. Holtrop F, Helling C, Lutz M, Van Leest K, De Bruin B, Slootweg C. Enhancement of London Dispersion in Frustrated Lewis Pairs: Towards a Crystalline Encounter Complex. *Synlett* 2022, **34**(10)**:** 1122-1128.

24. Rocchigiani L, Ciancaleoni G, Zuccaccia C, Macchioni A. Probing the Association of Frustrated Phosphine–Borane Lewis Pairs in Solution by NMR Spectroscopy. *J Am Chem Soc* 2014, **136**(1)**:** 112-115.

25. Bannwarth C, Hansen A, Grimme S. The Association of Two "Frustrated" Lewis Pairs by State-of-the-Art Quantum Chemical Methods. *Isr J Chem* 2015, **55**(2)**:** 235-242.

26. Mako TL, Racicot JM, Levine M. Supramolecular Luminescent Sensors. *Chem Rev* 2019, **119**(1)**:** 322-477.

27. Skorjanc T, Shetty D, Trabolsi A. Pollutant removal with organic macrocycle-based covalent organic polymers and frameworks. *Chem* 2021, **7**(4)**:** 882-918.

28. Olivo G, Capocasa G, Del Giudice D, Lanzalunga O, Di Stefano S. New horizons for catalysis disclosed by supramolecular chemistry. *Chem Soc Rev* 2021, **50**(13)**:** 7681-7724.

29. Thordarson P. Determining association constants from titration experiments in supramolecular chemistry. *Chem Soc Rev* 2011, **40**(3)**:** 1305-1323.

30. Sieland B, Stahn M, Schoch R, Daniliuc C, Spicher S, Grimme S, *et al.* Dispersion Energy-Stabilized Boron and Phosphorus Lewis Pairs. *Angew Chem Int Ed* 2023**:** e202308752.

31. Ashton PR, Boyd SE, Brindle A, Langford SJ, Menzer S, Pérez-García L, *et al.* Diazapyrenium-containing catenanes and rotaxanes. *New J Chem* 1999, **23**(6)**:** 587-602.

32. Welch GC, Stephan DW. Facile Heterolytic Cleavage of Dihydrogen by Phosphines and Boranes. *J Am Chem Soc* 2007, **129**(7)**:** 1880-1881.

33. Holtrop F, Jupp AR, Kooij BJ, van Leest NP, de Bruin B, Slootweg JC. Single-Electron Transfer in Frustrated Lewis Pair Chemistry. *Angew Chem Int Ed* 2020, **59**(49)**:** 22210-22216.

34. Holtrop F, Jupp AR, van Leest NP, Paradiz Dominguez M, Williams RM, Brouwer AM, *et al.* Photoinduced and Thermal Single-Electron Transfer to Generate Radicals from Frustrated Lewis Pairs. *Chem Eur J* 2020, **26**(41)**:** 9005-9011.

35. Brynn Hibbert D, Thordarson P. The death of the Job plot, transparency, open science and online tools, uncertainty estimation methods and other developments in supramolecular chemistry data analysis. *Chem Commun* 2016, **52**(87)**:** 12792-12805.

36. Bannwarth C, Ehlert S, Grimme S. GFN2-xTB—An Accurate and Broadly Parametrized Self-Consistent Tight-Binding Quantum Chemical Method with Multipole Electrostatics and Density-Dependent Dispersion Contributions. *J Chem Theory Comput* 2019, **15**(3)**:** 1652-1671.

37. Grimme S. Semiempirical GGA-type density functional constructed with a long-range dispersion correction. *J Comput Chem* 2006, **27**(15)**:** 1787-1799.

38. Grimme S, Ehrlich S, Goerigk L. Effect of the damping function in dispersion corrected density functional theory. *J Comput Chem* 2011, **32**(7)**:** 1456-1465.

39. Weigend F, Ahlrichs R. Balanced basis sets of split valence, triple zeta valence and quadruple zeta valence quality for H to Rn: Design and assessment of accuracy. *Phys Chem Chem Phys* 2005, **7**(18)**:** 3297-3305.

40. Chai JD, Head-Gordon M. Long-range corrected hybrid density functionals with damped atom-atom dispersion corrections. *Phys Chem Chem Phys* 2008, **10**(44)**:** 6615-6620.

41. Zhao Y, Truhlar DG. The M06 suite of density functionals for main group thermochemistry, thermochemical kinetics, noncovalent interactions, excited states, and transition elements: two new functionals and systematic testing of four M06-class functionals and 12 other functionals. *Theor Chem Acc* 2007, **120**(1-3)**:** 215-241.